Tropospheric ozone profiles from a ground-based ultraviolet spectrometer: a new retrieval method

Xiong Liu, Kelly Chance, Christopher E. Sioris, Michael J. Newchurch, and Thomas P. Kurosu

We present, to the best of our knowledge, a new method to retrieve tropospheric ozone (O_3) profiles from ground-based ultraviolet spectroscopic measurements. This method utilizes radiance spectra in the Huggins bands (i.e., 300–340 nm) measured at three off-axis angles (e.g., 45°, 75°, and 85°) normalized to direct-Sun irradiances or zenith-sky radiances with the total column O_3 derived from direct-Sun or zenith-sky measurements as a constraint. The vertical resolution of the retrieved O_3 values ranges from ~3 km near the surface to ~12 km at 20 km altitude. This method can be used to measure diurnal variation of tropospheric O_3 profiles and is complementary to the Umkehr method that mainly measures ozone profiles in the stratosphere.   © 2006 Optical Society of America

OCIS codes: 010.4950, 010.7030, 280.0280, 000.2170.

1. Introduction

Ozone (O_3) plays a key role in the chemical processes and energy budget of the troposphere.[1,2] Currently, ozonesonde, airborne *in situ* instruments, and light detection and ranging (lidar) are the main approaches to measure tropospheric O_3 at high vertical resolution. In addition, limited tropospheric O_3 can be measured from satellite-based instruments such as the Global Ozone Monitoring Experiment[3–7] (GOME) or ground-based measurements through the Umkehr method[8,9] but with coarser vertical resolutions of 10–15 km. Retrieving tropospheric O_3 from these passive remote sensing observations is a great challenge, because almost 90% of the total column O_3 (TCO) is in the stratosphere.

The first method for measuring O_3 profiles from ground-based measurements in the ultraviolet (UV) is the Umkehr method,[10,11] which is currently being used for routine observations of O_3 trends from both Dobson and Brewer instruments. In this method, ratios of zenith-sky radiances at two wavelengths in the UV, one strongly and the other weakly absorbed by O_3, are measured with the solar zenith angle (SZA) varying from 60° to 90° during morning and evening twilight.[8] Measured TCO from Dobson or Brewer measurements is used to constrain the ozone profile retrieval.[8] The Umkehr method mainly contains information about the vertical distribution of O_3 in the stratosphere, with about four independent pieces of information (i.e., significant eigenvectors) at 20–40 km.[12] Petropavlovskikh *et al.*[9] stated that approximately 1/4 of the information is actually below 20 km due to the TCO measurement, which was not considered in the information analysis of previous studies. Besides having limited information in the troposphere, the Umkehr observation lasts approximately 2 h and is restricted to the sunset and sunrise periods. Similar methods have been applied to measured NO_2 profiles from ground-based measurements along with photochemical models to model the temporal variation of this chemically active species.[13–16]

Jiang *et al.*[17] performed a theoretical study to derive tropospheric O_3 from ground-based measurements in the Huggins bands. Stratospheric O_3 contributes to direct irradiances and diffuse (including zenith and off-axis) radiances mainly by single scattering, while tropospheric O_3 contributes to direct irradiances by single scattering and to diffuse radiances mainly by multiple scattering. The ratios of diffuse radiances to direct irradiances provide a way to discriminate between tropospheric and stratospheric O_3. Zenith-sky, off-axis, and multiaxis differential optical absorption spectroscopy (MAXDOAS) techniques from ground-based UV–visible measurements have been used to measure trace gases (e.g.,

X. Liu (xliu@cfa.harvard.edu), K. Chance, C. E. Sioris, and T. P. Kurosu are with the Atomic and Molecular Physics Division, Harvard-Smithsonian Center for Astrophysics, Cambridge, Massachusetts 02138. M. J. Newchurch is with the Department of Atmospheric Science, University of Alabama in Huntsville, Huntsville, Alabama 35805.

NO_2, O_3, OClO, BrO, SO_2, IO, NO_3) since the early 1990s.[18] Hönninger et al.[18] demonstrated that vertical profile information of these trace gases in the lower troposphere can be retrieved from MAXDOAS measurements. Schofield et al.[19,20] combined both zenith-sky and direct-Sun measurements to measure both tropospheric and stratospheric BrO from ground-based instruments under various low-Sun conditions. In addition, off-axis measurements with an airborne UV–visible spectrometer have been used to retrieve trace gas concentrations. Petritoli et al.[21] measured O_3 concentrations near flight altitude from the measured UV spectra at three angles (one near zenith and two near horizon). An airborne version of the MAXDOAS (AMAXDOAS) instrument has been deployed to take UV–visible measurements in both down-looking and up-looking directions.[22] Bruns et al.[23] performed a theoretical study to show that profile information for NO_2 can be obtained from this instrument. Liu et al.[24] proposed mapping tropospheric O_3 profiles at high spatial resolutions (2 km × 2 km) and moderate vertical resolutions (2–6 km) from airborne UV–visible off-axis measurements normalized by direct irradiances or zenith-sky radiances at only two up-looking angles close to the horizon (e.g., 75° and 85°) and any down-looking angle. The up-looking measurements provide profiling information for O_3 above the aircraft and could be similarly taken from ground observations to derive height-resolved information above the ground. Jiang et al.[25] also demonstrated the possibility of retrieving tropospheric O_3 from both ground-based and spaceborne polarization measurements of scattered sunlight because the degree of linear polarization is ten times more sensitive to tropospheric O_3 than to stratospheric O_3. Hasekamp and Landgraf[26] showed that polarization measurements in addition to the reflection measurements significantly improve the vertical resolutions of retrieved tropospheric O_3.

This paper presents to our knowledge, a new method for retrieving tropospheric O_3 profiles from ground-based UV spectra in the Huggins bands (300–340 nm) at three viewing zenith angles (VZAs) using optimal estimation. This method refines the idea of using diffuse radiances and direct irradiances by Jiang et al.[17] to derive tropospheric O_3 profiles in the troposphere and extends the method of Liu et al.[24] from airborne UV spectra to ground-based UV spectra. TCO, simultaneously measured using the Dobson or Brewer method, is used to constrain the profile retrieval. This method can be used to measure O_3 in the troposphere and lower stratosphere with moderate vertical resolutions and is complementary to the Umkehr method, which mainly measures O_3 in the stratosphere. The focus of this study is to show the optimal performance of the O_3 profile retrieval using simulated radiance spectra under clear-sky conditions. We only consider ozone and background aerosols in the radiative transfer simulations and retrievals. Interferences due to the ring effect, undersampling, and other minor species (e.g., NO_2 and SO_2) are not considered; atmospheric conditions (e.g., temperature and aerosols) other than the O_3 profile are assumed to be known.

2. Methodology

O_3 profile retrieval from scattered or backscattered UV measurements is an ill-conditioned problem, i.e., there are no unique solutions for the measurements. Therefore we use the optimal estimation approach,[27] which uses climatological a priori information to stabilize the retrievals, to invert measurements, and to derive O_3 profiles. A simple description of the optimal estimation approach relevant to this study has been provided in Liu et al.[24] Readers are referred to Rodgers[27] for more details. The linearized discrete ordinate radiative transfer (LIDORT) model[28,29] is used as a forward model to simulate ground-based measurements and weighting functions. The version of LIDORT used here implements the pseudospherical approximation and neglects the effect of polarization on radiances. Although neglecting polarization can cause radiance errors of up to 10% in a pure Rayleigh atmosphere,[30] it does not affect the information analysis and retrievals from simulated measurements because polarization is neglected in both the simulation and the retrieval.

As a base case, simulations are performed using clear-sky conditions and the 1976 U.S. Standard Atmosphere. The O_3 profile for this atmosphere, which has a TCO of 345 Dobson units (1 DU= 2.687×10^{16} molecules cm^{-2}), is shown in Fig. 1. Tropospheric aerosols corresponding to a visibility of 50 km and background stratospheric aerosols from LOWTRAN[31] are used; the aerosol optical thickness is ∼0.14 at 550 nm. A surface albedo of 0.1 is assumed. A SZA of 45° and a relative azimuth zenith angle (AZA) of 90° are used. The proposed measurements of irradiances and diffuse radiances are taken in the ozone Huggins bands (e.g., 300–340 nm), in which the temperature-dependent O_3 absorption structure provides tropospheric O_3 information.[32] The slit function is assumed to have a Gaussian shape with a full width at half-maximum (FWHM) of 1.0 nm (i.e., spectral resolution), and a spectral sampling of 0.5 nm/pixel. The signal-to-noise ratios (SNR) in the simulated measurements are based on current detector technology, from ∼160 at 300 nm to 2000 at 340 nm for the above conditions. Random noise measurement errors, which depend on the simulated radiances, are added to the measurements before the inversions. The atmosphere is modeled on an Umkehr-type grid with 22 layers from 0 to ∼60 km, in steps of ∼2.5 km for each of the bottom 20 layers and ∼5 km for the top two layers. The tropopause height in the U.S. Standard Atmosphere, applied to the World Meteorological Organization (WMO) definition,[33] is 12 km. However, for convenient analysis, we assume that the tropopause is at 12.51 km (i.e., on the top of the fifth retrieval layer). The tropospheric column O_3 (TRCO) is 40.9 DU.

The a priori O_3 profile used in the retrievals and its standard deviations, shown in Fig. 1, are extracted from the Total Ozone Mapping Spectrometer (TOMS)
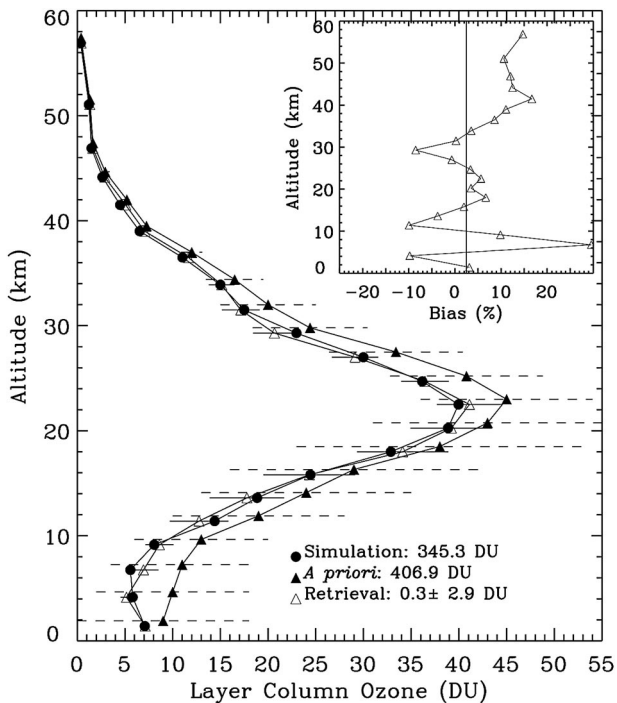
Fig. 1. Simulated (1976 U.S. Standard Atmosphere), *a priori*, and retrieved O_3 profiles for the base case. The *a priori* standard deviations are plotted as dashed error bars and the retrieval errors (instrument random noise + smoothing) are plotted as solid error bars. For clarity, the *a priori* profile is shifted upward by 0.5 km. The inset shows the relative difference between the retrieved and the simulated profiles. The TCO for the simulated and *a priori* profiles is indicated and the bias and retrieval error in the TCO are indicated for the retrieved profile.

version-8 climatology[34] in mid-latitude winter with the following modification. To show the strong sensitivity of our method to O_3 in the troposphere and lower stratosphere, we move the *a priori* profile far away from the simulated O_3 profile in those altitude regions. To extract more available information from the measurements, we relax the *a priori* constraint by increasing the original *a priori* standard deviations in the troposphere. A correlation length of 5 km is used to construct the *a priori* covariance matrix for the whole atmosphere.

The concept of the air mass factor (AMF) has been widely used for interpreting scattered-light DOAS observations.[18,35] The AMF is usually defined as the ratio of the slant column density to the vertical column density, or the average photon path length in the atmosphere to the vertical thickness of the atmosphere. We similarly apply the AMF concept for each layer to interpret the measurements, so the AMF used here is defined as the ratio of the average photon path length in a particular atmospheric layer of all photons detected by the spectrometer to the vertical thickness of that layer. The AMF is derived from LIDORT weighting functions using the approach described in Liu *et al.*[24] Figure 2(a) shows the AMFs for direct irradiances and radiances at several VZAs and at 310 and 340 nm for the base case. The AMF for the direct irradiance is just the geometric AMF, i.e., con-
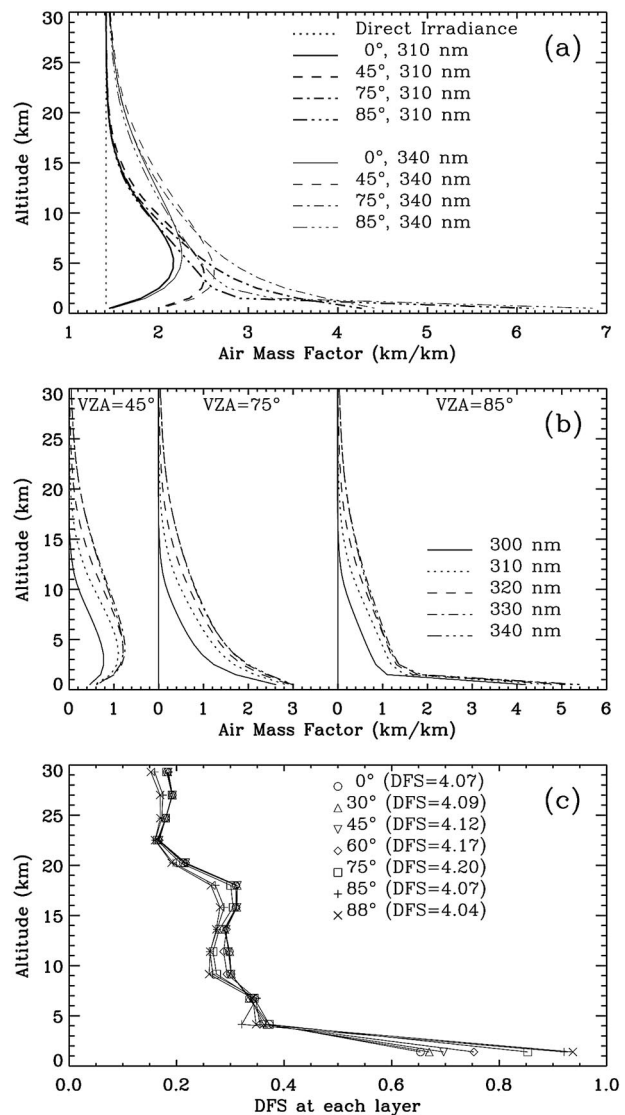

Fig. 2. (a) AMFs for radiances at 310 and 340 nm for zenith and three VZAs (45°, 75°, and 85°) and direct-Sun irradiance. (b) AMFs for normalized radiances at 300, 310, 320, 330, and 340 nm for VZAs of 45°, 75°, and 85°. (c) Profiles of DFS using radiance spectra at VZAs of 0°, 30°, 45°, 60°, 75°, 85°, and 88°. The total DFS is also shown in parentheses. Surface albedo is assumed to be 0.1 and the SZA is 45°.

stant with altitude. At altitudes greater than ~20–25 km, the AMFs for zenith-sky radiances are close to the geometric AMF, indicating that those photons tend to traverse these layers as part of the direct solar radiation. With decreasing altitude, those photons experience multiple scattering events and the AMF increases until the extinction along the path prevents them from reaching the detector. The peaking altitude in AMF for zenith sky is at 5.5 km for both 310 and 340 nm, suggesting that the zenith-sky measurement is most sensitive to O_3 at this altitude. Below the peaking altitude, only photons that experience fewer scattering events can reach the detector from the zenith-sky direction because of the strong Rayleigh and aerosol scattering near the sur-

face and therefore the AMF decreases. With increasing VZA, the peaking altitude decreases (e.g., 3.5 and 4.5 km for a VZA of 45° at 310 and 340 nm, respectively) because of the increasing extinction along the longer path in the line of sight; the peak magnitude increases also because of the longer path in the line of sight. At VZAs of 75° and 85°, the AMFs peak at the bottom layer. At longer wavelengths, there is usually less extinction along the path, and photons experience more multiple scattering at higher altitudes. Both the peaking magnitude and altitude increase. Therefore measurements at smaller VZAs and longer wavelengths (i.e., less absorption) provide more sensitivity to O_3 at higher altitudes.

Remote sensing of O_3 and other species typically requires a solar reference spectrum to normalize the radiances. Similar to Liu *et al.*,[24] the direct irradiance or the zenith-sky radiance can serve this purpose. We can see from Fig. 2(a) that using a direct-Sun reference increases sensitivity to O_3 and to O_3 at higher altitudes. Therefore we use the direct-irradiance reference in the base case. However, using normalization removes the sensitivity to O_3 at higher altitudes, so the retrieval is insensitive to ozone at those altitudes and TCO. In the Dobson or Brewer measurements, TCO is derived from zenith-sky or direct-Sun measurements at one or several wavelength pairs.[36] In our method the measurements needed for TCO retrieval are available from either the zenith-sky radiance or direct-Sun irradiance spectrum after performing absolute radiance calibration. Similar to the Umkehr method,[8] we use the derived TCO to constrain the ozone profile retrieval and to provide sensitivity to O_3 at high altitudes. It is treated as one element of the measurement vector; the measurement error in TCO is assumed to be 3 DU following Mateer and Deluisi.[8] The difference between the integrated TCO from the O_3 profile and the constrained TCO is then minimized in the retrievals simultaneously with those between measured and simulated radiances.

Figure 2(b) shows the AMFs at VZAs of 45°, 75° and 85° for radiances normalized by direct irradiances at five selected wavelengths. As in Liu *et al.*,[24] AMFs are wavelength and altitude dependent at all VZAs, therefore showing O_3 profiling information in the troposphere and lower stratosphere. If the zenith-sky reference is used, the normalized radiances will contain less profiling information because the normalized AMFs are smaller. To compare the available information content at different VZAs, we perform the retrievals from ground-based UV spectra under different VZAs. Figure 2(c) compares the degrees of freedom for signal [(DFS), i.e., the number of pieces of information in the measurements] at each retrieval layer. The differences in total DFS are within 0.2 over the VZA range. For the first layer near the surface, the DFS is larger for larger VZAs. At higher layers, the DFS is usually slightly worse for larger VZAs. The variation in DFS versus VZA is consistent with the analysis in Figs. 2(a) and 2(b). The differences suggest that we could combine mea-

surements at different VZAs to improve the retrievals. Different combinations of VZAs are tested and we find that the combination of 45°, 75°, and 85° gives the best retrieval, with a total DFS of 5.6. Using additional measurements from other VZAs improves the retrieval minimally. In the base case we combine measurements taken at VZAs of 45°, 75°, and 85°.

3. Results and Discussion

Figure 3 shows the retrieval averaging kernels (AKs) for four cases. To show how the constraint contributes to the retrieval, we show the AKs for the base case except without the TCO constraint ("no TCO constraint") in Fig. 3(a). Figure 3(b) shows the AKs for the base case. To compare the height-resolved O_3 information from this method with that of the Umkehr method, Fig. 3(c) shows the AKs for the standard Umkehr method, which takes measurements at 12 SZAs ranging from 60° to 90°. Although the measurement random errors increase with SZA,[9] we assume them to be 0.7 N value (i.e., relative logarithmic attenuation for the wavelength pair in 100 log units) in the normalized N values and to be independent of SZA, as was used in Petropavlovskikh *et al.*[9] Because LIDORT cannot calculate radiances at a SZA of 90°, we use 89.9°. Furthermore, we show in Fig. 3(d) the AKs of combining our proposed and Umkehr measurements ("combined") to demonstrate how the information in the Umkehr and our proposed method is complementary.

For the "no TCO constraint" case, the total DFS is 4.9 with 3.3 in the troposphere and 4.5 below 20.3 km, suggesting the retrieval is particularly sensitive to tropospheric O_3 and to a lesser degree to lower stratospheric O_3. For the bottom three layers, the individual DFS is greater than 0.6; the kernels are sharply peaked with vertical resolutions of 2.8, 2.9, and 4.3 km FWHM at 1.4, 4.2, and 6.8 km, respectively. With increasing altitude to 20.3 km, the peaking altitudes of AKs usually agree with the actual altitudes, but some shift to adjacent altitudes because of broad peaks, and the vertical resolution decreases (e.g., 11.5 km at 20.3 km). Above 22.5 km the peaks of the AKs largely shift to 20.3 or 22.5 km and the peak magnitudes decrease with increasing altitudes. There is hardly any sensitivity to O_3 above 30 km. After adding the TCO constraint (base case), the AKs are almost the same, with the same DFS in the troposphere [Fig. 3(b)]. The major change occurs at altitudes greater than ~22.5 km where the AKs appear to be flat, indicating there is no profiling information, but only column O_3 information above that altitude. Correspondingly, the increase in total DFS by 0.7 mostly comes from altitudes above 22.5 km.

For the Umkehr method [Fig. 3(c)], the vertical resolutions are in the range of 10–15 km from surface to ~35 km. Above 35 km, the AKs are flatter because of less height-resolved information and mainly the TCO information. AKs for the bottom four layers that peak near the surface are also mainly due to the TCO constraint. The retrievals are most sensitive to O_3 at 22–35 km with vertical resolutions of ~10 km. The
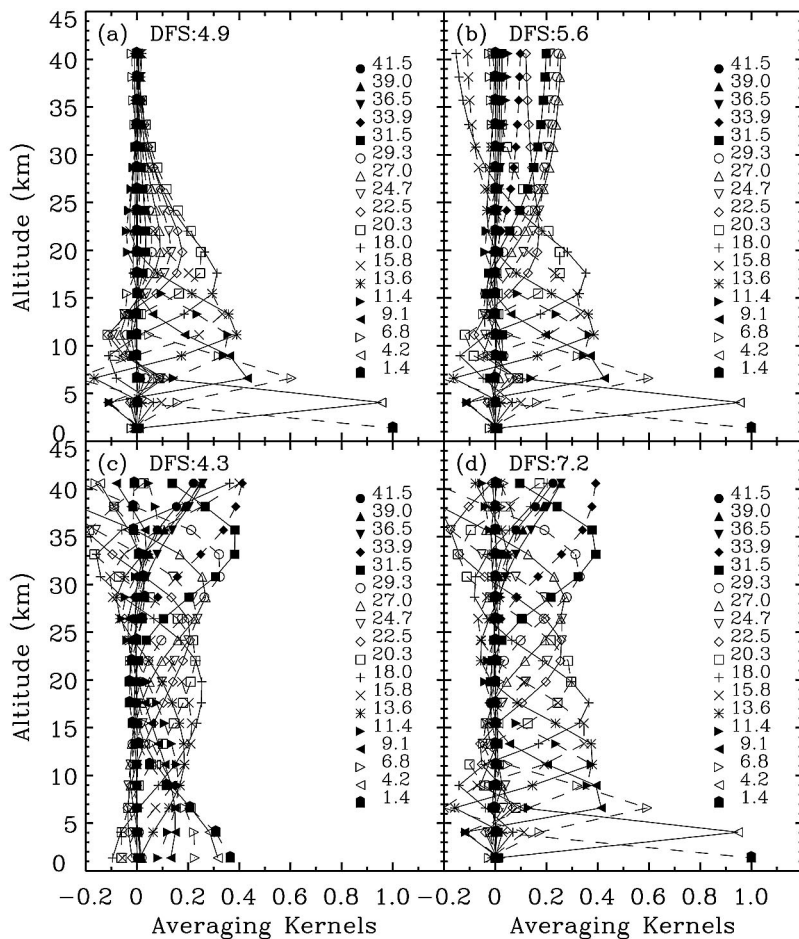
Fig. 3. Averaging kernels for using (a) the base case except without total column O_3 constraint, (b) base case, (c) Umkehr method, and (d) combination of Umkehr and our proposed approach. The total DFS is listed. Each line refers to the sensitivity of retrieved O_3 at the layer indicated in the legend to the perturbed O_3 at each layer.

total DFS is 4.3, of which 3.2 is in the stratosphere. Note that the AKs are slightly different from those in the operational algorithms because of different measurement errors and the *a priori* covariance matrix. The operational Umkehr method uses the uniform *a priori* covariance matrix (25% uncertainty at each level) for the purpose of trend analysis.[8]

For the combined case [Fig. 3(d)], we can clearly see the improvement in the information content. The vertical resolutions from surface to ~35 km are within 11 km and the AKs usually peak at their own altitudes. The total DFS is 7.2 with the same tropospheric DFS of 3.3 as Fig. 3(a), suggesting that tropospheric O_3 information is mostly provided from our new method. Compared to the Umkehr retrieval, the improvement occurs not only in the troposphere but also in the stratosphere, with stratospheric DFS increasing from 3.2 to 3.9.

Although the Umkehr method takes approximately 2 h and is restricted to sunset and sunrise periods, it is mainly sensitive to O_3 in the stratosphere, where O_3 has less variability during the day. Our proposed method is mainly sensitive to O_3 in the troposphere, where O_3 has more variability, and the measurements can be taken within a short time period relative to the Umkehr method, so the diurnal variation of the tropospheric O_3 can be captured. However, the information in the stratosphere is relatively poor. Therefore our proposed method and the Umkehr method are complementary by providing information on different altitude regions. Furthermore, when we take the measurements using our proposed method during the day (including zenith-sky radiances), we will have the measurements required for Umkehr retrieval. In practice, we can use the retrieved O_3 profile from the Umkehr method as *a priori* for our proposed method, but assign smaller *a priori* standard deviations to altitude ranges where O_3 information is mostly contributed from the Umkehr technique.

Figure 1 shows the retrieved profile and retrieval errors resulting from instrument random noise (i.e., precision) and smoothing for the base case using the proposed method [i.e., Fig. 3(b)]. The inset to Fig. 1 shows the relative biases between retrieved and simulated values. Table 1 shows the biases and retrieval errors in the TCO, TRCO, and stratospheric column O_3 (SCO) and the DFS in the whole atmosphere and troposphere for the base case. The retrieval errors are based on the formulation in Rodgers.[27] We derive smoothing errors with a real covariance matrix[27] (different from the *a priori* covariance matrix), which is derived from 23 years (1980–2002) of ozonesonde measurements at Hohenpeissenberg in January (for 0–30 km) and from SAGE data (for 30–60 km).
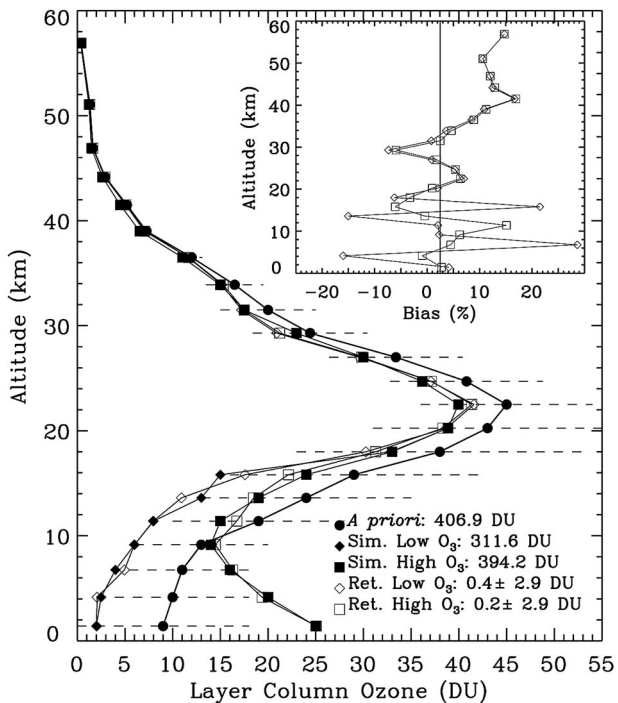
Fig. 4. Similar to Fig. 1 but for retrievals under two modified scenarios, representing low and high tropospheric O_3 conditions, respectively.

Retrieved O_3 values agree well with the simulated values; within 2 DU at each layer. There are large alternating negative or positive relative biases of up to 25% in layers 2–5 from the bottom because the partial column O_3 at those layers is small, and the vertical resolution of 3–8 km is not adequate to resolve each individual layer. There are large systematic positive biases of 6%–13% above 31.5 km due to limited information above this altitude. The fraction of retrieval errors to *a priori* errors is <1% for the first layer, <10% for the second layer, and increasing to >40% at altitude 20 km, suggesting that this method provides reliable information mainly below 20 km. Above 20 km, the information is mainly from the TCO constraint and the *a priori* profile shape. The bias in TRCO is less than 0.5 DU (1.5%) and its retrieval error is 2.3 DU (5.6%). The bias in SCO is within 1 DU (0.3%) with a retrieval error of 3.6 DU (1.2%).

Table 1 also shows the retrievals for the other three cases in Fig. 3. Without the TCO constraint, there are large biases and retrieval errors in the TCO and SCO, consistent with the analysis in Fig. 3. However, TRCO is still well retrieved as in the base case. When the Umkehr method is used, the retrieval errors in the troposphere and stratosphere are larger than those for the base case because the information in the Umkehr method is relatively weak in the upper troposphere and lower stratosphere region. With combined measurements, the retrieval uncertainties in TCO, SCO, and TRCO are reduced.

Figure 4 shows the retrieved profiles for two scenarios having low and high amounts of tropospheric O_3, respectively, using our method. These simulated profiles are only modified from the simulated profile in the base case in the lowest seven layers. The low tropospheric O_3 scenario has a TRCO of 22.5 DU and has an average O_3 mixing ratio of ~10 parts/billion by volume (ppbv) in the near-surface layer; the high tropospheric O_3 scenario has a TRCO of 90.0 DU and has an average O_3 mixing ratio of ~125 ppbv in the near-surface layer. The retrieved profiles agree well with the simulated profiles for both scenarios. Although *a priori* values are very different from the actual values near the surface, the retrieved values are within 3 DU (30%) of the simulated values in the troposphere. The good agreement demonstrates the strong sensitivity of this method to tropospheric O_3. The biases in TRCO are within 2 DU (2%) and the retrieval errors are within 3.4 DU (11%). The biases in SCO are within 3 DU (1%) and the retrieval uncertainties are less than 3.6 DU (1.3%).

We have carried out sensitivity studies of this approach to reference normalization, spectral resolution, wavelength range, measurement error, surface albedo, and viewing geometry on the base case (Table 1). When the zenith-sky reference is used, the retrieved information is slightly reduced in both the stratosphere and the troposphere as expected from Fig. 2(a). In practice, the zenith-sky reference has certain advantages over the direct-Sun reference since the information is only slightly reduced. Zenith-sky radiances can be measured together with other off-axis scattered measurements using the exact same optical devices and hence no Sun tracker, diffuser plate, and rotating shadowband devices are needed. In addition, normalization to the zenith-sky reference will provide better radiometric calibration without the need to calibrate additional optical components such as a diffuser plate. Unlike the previous airborne method,[24] using an external solar reference spectrum measured at the top of the atmosphere only slightly improves the retrieval because the solar irradiance mainly provides the TCO information, which is already utilized in the retrieval from the TCO constraint. This method does not require very high spectral resolution; increasing the spectral resolution from 1.0 to 0.2 nm FWHM and increasing the spectral sampling from 0.5 to 0.1 nm/pixel increases the DFS only by ~0.2 in both the troposphere and the stratosphere. Including measurements in the Chappuis bands only slightly improves the retrieval. Tropospheric ozone can still be well retrieved when the shortest wavelength is changed from 300 to 310 or 320 nm, although the retrieval uncertainties increase and the DFS in the troposphere and stratosphere decrease by ~0.2 each for using fitting window 310–340 nm, and by ~0.6 and ~0.4, respectively, for using fitting window 320–340 nm. If the SNR is reduced by a factor of 10, the DFS is reduced by 0.7 and 0.8 in the stratosphere and troposphere, respectively, and tropospheric O_3 can still be measured at moderate vertical resolution, with a tropospheric DFS of 2.5. The method performs slightly better for high surface albedo. At large SZA, the performance of the method strongly depends on

Table 1. Column O₃ Biases and Retrieval Errors[a]

| Cases[b] | Biases and Retrieval Errors (DU) | | | DFS |
	Total	Tropospheric	Stratospheric	Total/Tropospheric
Base case	0.3 ± 2.9	-0.3 ± 2.3	0.6 ± 3.6	5.6/3.3
No TCO constraint	8.4 ± 10.7	0.2 ± 2.5	8.2 ± 10.1	4.9/3.3
Umkehr[c]	0.4 ± 2.9	-2.4 ± 6.2	2.9 ± 5.4	4.3/1.1
Combined	1.4 ± 1.7	0.0 ± 2.2	1.4 ± 2.7	7.2/3.3
High tropospheric O₃	0.2 ± 2.9	1.9 ± 2.5	-1.7 ± 3.6	5.2/3.0
Low tropospheric O₃	0.4 ± 2.9	0.5 ± 2.3	-0.1 ± 3.5	5.7/3.3
Zenith reference	0.3 ± 2.9	0.1 ± 3.1	0.2 ± 4.3	5.0/3.1
Solar reference	0.6 ± 0.5	-1.6 ± 2.3	2.3 ± 2.5	5.7/3.2
0.2-nm FWHM, 0.1 nm/pixel	0.1 ± 2.9	-0.3 ± 2.2	0.4 ± 3.4	6.0/3.5
Include Chappuis bands[d]	0.4 ± 2.9	-0.2 ± 2.3	0.7 ± 3.5	5.8/3.4
Wavelength range 310–340 nm	0.5 ± 2.9	-0.9 ± 2.3	1.3 ± 3.6	5.2/3.1
Wavelength range 320–340 nm	0.2 ± 2.9	2.4 ± 3.8	-2.2 ± 4.8	4.6/2.7
Ten times worse SNR	0.0 ± 3.0	2.5 ± 4.0	-2.5 ± 5.0	4.1/2.5
Surface albedo 0.6	0.3 ± 2.9	-0.6 ± 2.3	0.2 ± 3.5	5.7/3.3
SZA 0°	0.4 ± 2.9	-0.6 ± 2.3	1.0 ± 3.5	5.8/3.4
SZA 75°	0.0 ± 1.9	0.2 ± 5.3	-0.2 ± 5.6	4.7/2.3
SZA 85°[e]	-0.2 ± 1.9	-1.2 ± 4.0	0.9 ± 4.7	4.5/2.1
AZA 0° (i.e., solar side)	0.3 ± 2.9	-0.2 ± 2.4	0.5 ± 3.6	5.5/3.2
AZA 180° (i.e., antisolar side)	0.3 ± 2.9	-0.3 ± 2.4	0.6 ± 3.6	5.6/3.3

[a]Due to measurement random noise and smoothing in total, tropospheric, and stratospheric column O₃, and total and tropospheric DFS for different atmospheric scenarios and instrument designs. The biases are the differences between retrieved and simulated values.
[b]The descriptions in this first column list the difference compared to the base case unless specified.
[c]The Umkehr method is used with the same *a priori* profile and covariance matrix.
[d]1.1 nm FWHM spectral resolution and 3 nm/pixel sampling rate from 530 to 650 nm.
[e]Only 310–340 nm is used because measurements below 310 nm have large measurement errors and do not contribute to the retrieval.

SZA. The performance at SZAs of 0° and 45° does not differ much. However, when the SZA increases from 45° to 75° or 85°, the DFS decreases by ~1, most of which occurs in the troposphere, and retrieval uncertainties in TRCO and SCO increase. The method works almost equally well under different AZAs, and the DFS and the retrieval uncertainties are similar for different AZAs.

4. Conclusions

We describe to our knowledge, a new retrieval method for measuring tropospheric O₃ profiles from ground-based ultraviolet spectrometer measurements. The profile retrieval uses radiance spectra at three viewing zenith angles (e.g., 45°, 75°, and 85°) normalized to the direct-Sun irradiances or zenith-sky radiances with the TCO derived from zenith-sky radiances or direct-Sun irradiances as a constraint. The profiling takes advantage of the wavelength-dependent and altitude-dependent photon path lengths, which is in turn caused by the complex interplay between scattering and extinction, and the temperature-dependent O₃ absorption structure in the Huggins bands. The vertical resolution of retrieved O₃ ranges from ~3 km near the surface to ~12 km at 20 km. The height-resolved O₃ information at higher altitudes is weak; column O₃ information can mainly be measured through the simultaneously retrieved TCO. This method can be used to measure the diurnal variation of tropospheric O₃ and lower stratospheric O₃ at moderate vertical resolution. It is complementary to the Umkehr method by providing O₃ profile information in the troposphere.

References

1. G. P. Brasseur, J. T. Kiehl, J.-F. Muller, T. Schneider, C. Granier, X. X. Tie, and D. Hauglustaine, "Past and future changes in global tropospheric ozone: impact on radiative forcing," Geophys. Res. Lett. **25,** 3807–3810 (1998).
2. P. J. Crutzen, "Tropospheric ozone: an overview," in *Tropospheric Ozone, Regional, and Global Scale Interaction,* NATO ASI Series, D. Reidel, ed. (Springer, 1988), pp. 3–32.
3. R. Munro, R. Siddans, W. J. Reburn, and B. Kerridge, "Direct measurement of tropospheric ozone from space," Nature **392,** 168–171 (1998).
4. R. Hoogen, V. V. Rozanov, and J. P. Burrows, "Ozone profiles from GOME satellite data: algorithm description and first validation," J. Geophys. Res. **104,** 8263–8280 (1999).
5. O. P. Hasekamp and J. Landgraf, "Ozone profile retrieval from backscattered ultraviolet radiances: the inverse problem solved by regularization," J. Geophys. Res. **106,** 8077–8088 (2001).
6. R. J. van der A, R. F. van Oss, A. J. M. Piters, J. P. F. Fortuin, Y. J. Meijer, and H. M. Kelder, "Ozone profile retrieval from recalibrated GOME data," J. Geophys. Res. **107,** 4239, doi:10.1029/2001JD000696 (2002).
7. X. Liu, K. Chance, C. E. Sioris, R. J. D. Spurr, T. P. Kurosu, R. V. Martin, and M. J. Newchurch, "Ozone profile and tropospheric ozone retrievals from global ozone monitoring experi-

ment: algorithm description and validation," J. Geophys. Res. **110,** D20307, doi:10.1029/2005JD006240 (2005).

8. C. L. Mateer and J. J. Deluisi, "A new Umkehr inversion algorithm," J. Atmos. Terr. Phys. **54,** 537–556 (1992).

9. I. Petropavlovskikh, P. K. Bhartia, and J. DeLuisi, "An improved Umkehr algorithm," NOAA Cooperative Institute for Research in Environmental Sciences, 2004, http://www.srrb.noaa. gov/research/umkehr/append_umk_pdf.pdf

10. F. W. P. Gotz, "Zum Strahlungsklima des Spitzbergensommers. Strahlugns-und Ozonmessungen in der Konigsbucht 1929," Gerlands Beltr. **31,** 119–154 (1931).

11. F. W. P. Gotz, A. R. Meetham, and G. M. B. Dobson, "The vertical distribution of ozone in the atmosphere," Proc. R. Soc. London Ser. A **145,** 416–446 (1934).

12. C. L. Mateer, "On the information content of Umkehr observations," J. Atmos. Sci. **22,** 370–381 (1965).

13. J. F. Noxon, E. C. Whipple, Jr., and R. S. Hyde, "Stratospheric NO_2 1. Observation method and behavior at mid-latitude," J. Geophys. Res. **84,** 5047–5065 (1979).

14. R. L. McKenzie, P. V. Johnston, C. T. McElroy, J. B. Kerr, and S. Solomon, "Altitude distributions of stratospheric constituents from ground-based measurements at twilight," J. Geophys. Res. **96,** 15499–15511 (1991).

15. K. E. Preston, R. L. Jones, and H. K. Roscoe, "Retrieval of NO_2 vertical profiles form ground-based UV-visible measurements: method and validation," J. Geophys. Res. **102,** 19089–19097 (1997).

16. K. E. Preston, D. J. Fish, H. K. Roscoe, and R. L. Jones, "Accurate derivation of total and stratospheric vertical columns of NO_2 from ground-based zenith-sky measurements," J. Atmos. Chem. **30,** 163–172 (1998).

17. Y. Jiang, Y. L. Yung, and S. P. Sander, "Detection of tropospheric ozone by remote sensing from the ground," J. Quant. Spectrosc. Radiat. Transfer **57,** 811–818 (1997).

18. G. Hönninger, C. von Friedeburg, and U. Platt, "Multi axis differential optical absorption spectroscopy," Atmos. Chem. Phys. **4,** 231–254 (2004), and references therein.

19. R. Schofield, B. J. Connor, K. Kreher, and P. V. Johnston, "The retrieval of profile and chemical information from ground-based UV-visible spectroscopic measurements," J. Quant. Spectrosc. Radiat. Transfer **86,** 115–131 (2004).

20. R. Schofield, K. Kreher, B. J. Connor, P. V. Johnston, A. Thomas, D. Shooter, M. P. Chipperfield, C. D. Rodgers, and G. H. Mount, "Retrieved tropospheric and stratospheric BrO columns over Lauder, New Zealand," J. Geophys. Res. 109, doi:10.1029/2003JD004463 (2004).

21. A. Petritoli, F. Ravegnani, G. Giovanelli, D. Bortoli, U. Bonafe, I. Kostadinov, and A. Oulanovsky, "Off-axis measurements of atmospheric trace gases by use of an airborne ultraviolet–visible spectrometer," Appl. Opt. **41,** 5593–5599 (2002).

22. T. Wagner, M. Bruns., J. P. Burrows, S. Fietkau, F. Finocchi, K.-P. Heue, G. Honninger, U. Platt, I. Pundt, A. Richter, R. Rollenbeck, C. v. Friedeburg, F. Wittrock, and P. Xie, "The AMAXDOAS instrument and its application for SCIAMACHY validation," presented at the 15th ESA Symposium on European Rocket and Balloon Programs and Related Research, Biarritz, France, May 28–31, 2001.

23. M. Bruns, S. A. Buehler, J. P. Burrows, K.-P. Heue, U. Platt, I. Pundt, A. Richter, A. Rozanov, T. Wagner, and P. Wang, "Retrieval of profile information from airborne multiaxis UV/visible skylight absorption measurements," Appl. Opt. **43,** 4415–4426 (2004).

24. X. Liu, C. E. Sioris, K. Chance, T. P. Kurosu, M. J. Newchurch, R. V. Martin, and P. I. Palmer, "Mapping tropospheric ozone profiles from an airborne UV/visible spectrometer," Appl. Opt. **44,** 3312–3319 (2005).

25. Y. Jiang, Y. L. Yung, S. P. Sander, and L. D. Travis, "Modeling of atmospheric radiative transfer with polarization and its application to the remote sensing of tropospheric ozone," J. Quant. Spectrosc. Radiat. Transfer **84,** 169–179 (2003).

26. O. P. Hasekamp and J. Landgraf, "Tropospheric ozone information from satellite-based polarization measurements," J. Geophys. Res. **107,** 4326, doi:10.1029/2001JD001346 (2002).

27. C. D. Rodgers, *Inverse Methods for Atmospheric Sounding: Theory and Practice* (World Scientific Publishing, 2000).

28. R. J. D. Spurr, T. P. Kurosu, and K. V. Chance, "A linearized discrete ordinate radiative transfer model for atmospheric remote-sensing retrieval," J. Quant. Spectrosc. Radiat. Transfer **68,** 689–735 (2001).

29. R. J. D. Spurr, "Simultaneous derivation of intensities and weighting functions in a general pseudo-spherical discrete ordinate radiative transfer treatment," J. Quant. Spectrosc. Radiat. Transfer **75,** 129–175 (2002).

30. M. I. Mishchenko, A. A. Lacis, and L. D. Travis, "Errors induced by the neglect of polarization in radiance calculations for Rayleigh scattering atmospheres," J. Quant. Spectrosc. Radiat. Transfer **51,** 491–510 (1994).

31. F. X. Kneizys, E. P. Shettle, L. W. Abreu, J. H. Chetwynd, G. P. Anderson, W. O. Gallery, J. E. A. Selby, and S. A. Clough, "Users Guide to LOWTRAN 7," AFGL-TR-88-0177 (Air. Force Geophysics Laboratory, Hanscom AFB, Mass., 1988).

32. K. V. Chance, J. P. Burrows, D. Perner, and W. Schneider, "Satellite measurements of atmospheric ozone profiles, including tropospheric ozone, from ultraviolet/visible measurements in the nadir geometry: a potential method to retrieve tropospheric ozone," J. Quant. Spectrosc. Radiat. Transfer **57,** 467–476 (1997).

33. WMO (World Meteorology Organization), "Definition of the tropopause," WMO Bull. **6,** 136 (1957).

34. R. D. McPeters, J. A. Logan, and G. J. Labow, "Ozone climatological profiles for version 8 TOMS and SBUV retrievals," presented at the American Geophysical Union Fall meeting, San Francisco, Calif. Dec. 7–12, 2003.

35. S. Solomon, A. L. Schmeltekopf, and R. W. Sanders, "On the interpertation of zenith sky absorption measurements," J. Geophys. Res. **92,** 8311–8319 (1987).

36. H. De Backer and D. De Muer, "Intercomparison of total ozone data measured with Dobson and Brewer ozone spectrophotometers at Uccle (Belgium) from January 1984 to March 1991 including zenith sky observations," J. Geophys. Res. **96,** 20711–20719 (1991).